MALAT1 modulates granulosa cells ferroptosis and apoptosis through PAK2 upregulation in polycystic ovary syndrome

Yun Yang[A,B,F], Dan Li[B,C], Lu Sun[C,D], Shasha Liu[D,E]

Department of Gynecology, Tianjin Central Hospital of Gynecology Obstetrics, China

A – research concept and design; B – collection and/or assembly of data; C – data analysis and interpretation;
D – writing the article; E – critical revision of the article; F – final approval of the article

Address for correspondence
Yun Yang
E-mail: erff5623@126.com

Conflict of interest
None declared

Abstract

Background. Polycystic ovary syndrome (PCOS) is a complicated endocrinological disorder.

Objectives. We investigated the ferroptosis-regulated role of MALAT1 and its potential modulatory mechanisms in granulosa cells (GCs).

Materials and methods. Reverse transcripton quantitative polymerase chain reaction (RT–qPCR) was used to measure the relative expression of MALAT1/miR-155-5p/PAK2 in KGN cells after transfection. Online bioinformatic analysis was performed to predict the interactions between MALAT1/PAK2 and miR-155-5p. Dual luciferase assays were performed for relative luciferase activity in cell groups co-transfected with the pmiRGLO plasmids containing wild type (wt) or mutant type (mt) of MALAT1 (MALAT1-wt, MALAT1-mt), siRNA targeting MALAT1(si-MALAT1) miR-155-5p inhibitor or their control was transfected into KGN cells using Lipofectamine 2000. After 48 h, the transfected cells were collected for the following experiments. Cell viability and apoptosis were measured using Cell Counting Kit-8 (CCK-8) and flow cytometry. Malondialdehyde (MDA) level and reduced glutathione (GSH) / oxidized glutathione disulfide (GSSG) ratio were detected using commercial kits. Western blot was used to measure the relative protein changes in PAK2, SLC7A11 and GPX4.

Results. Knockdown of MALAT1 decreased cell viability, increased apoptosis and ferroptosis, which was reversed by miR-155-5p inhibition. MALAT1 downregulation inhibited PAK2, while miR-155-5p inhibition activated PAK2. The increase of relative luciferase activity in cells transfected with MALAT1-wt or PAK2-wt and miR-155-5p inhibitor suggests the bindings between miR-155-5p and MALAT1 or PAK2.

Conclusions. This study revealed a novel ferroptosis-modulated role of MALAT1 in PCOS in vitro via interactions with miR-155-5p/PAK2. Further in vivo and clinical studies are needed to validate these in vitro findings and fully assess the therapeutic potential of MALAT1 in PCOS.

Key words: PCOS, ferroptosis, MALAT1, PAK2

Highlights

- MALAT1 controls ferroptosis in KGN granulosa cells, uncovering a novel lncRNA-driven cell-death pathway in ovarian physiology.
- Reduced MALAT1 expression links to polycystic ovary syndrome (PCOS)-associated ovarian dysfunction, highlighting its potential as a biomarker and therapeutic target in PCOS.
- MALAT1 sponges miR-155-5p to upregulate PAK2 in KGN cells, defining a MALAT1/miR-155-5p/PAK2 ceRNA network critical for granulosa-cell function.

Background

Polycystic ovary syndrome (PCOS) is a complex endocrinological disorder affecting 8–13% of reproductive-aged women worldwide, with approx. 70% of cases remaining undiagnosed.[1,2] As an ovulatory disorder, PCOS is characterized by irregular menstrual patterns, metabolic disturbances and hyperandrogenism. However, the precise causes of PCOS remain unclear, and there is an urgent need for accurate and efficient diagnostic methods.[3,4] Beyond known risk factors such as obesity, elevated testosterone levels and male-pattern balding, previous studies have reported numerous genetic and protein alterations in patients with PCOS.[5,6] An increasing body of research suggests that noncoding RNAs may play an important role in the pathogenesis of PCOS.[7] For example, long non-coding RNA (lncRNA) BBOX1 antisense RNA1 (AS1) has been found to be upregulated in the follicular fluid of PCOS patients and is known to promote the proliferation of granulosa cells (GCs) by downregulating miR-19b.[8] LncRNA HLA-F-AS1 is downregulated, while microRNA-613 expression is increased in the follicular fluid of PCOS patients; overexpression of HLA-F-AS1 has been shown to promote GC proliferation by inhibiting miR-613.[9] Metastasis-associated lung adenocarcinoma transcript-1 (MALAT1) has been found to be downregulated in peripheral blood leukocytes from obese PCOS patients[10] and similarly decreased in GCs from PCOS patients.[11,12] Previous studies have demonstrated that, in vitro, MALAT1 can regulate the viability and apoptosis of GCs and the human granulosa-like tumor cell line (KGN).[13] In PCOS rat models, MALAT1 is also downregulated in ovarian tissues, and upregulation of MALAT1 has been shown to protect against PCOS via the miR-302d-3p/LIF axis.[14] Mechanistically, MALAT1 modulates KGN cells and GCs in vitro through miR-125b/miR-203a/TGFβ signaling pathways.[12] In GCs and KGN cells, MALAT1 promotes the degradation and ubiquitination of p53, thereby regulating cell proliferation and apoptosis.[15] Recently, increased ferroptosis has been identified as being correlated with PCOS.[7,16] Ferroptosis in PCOS is associated with impaired mitochondrial dynamics, overproduction of proinflammatory cytokines and elevated oxidative stress.[17] In PCOS rat models, inhibition of ferroptosis has

been shown to significantly alleviate PCOS symptoms.[7,18] However, it remains unknown whether MALAT1 plays a role in mediating ferroptosis in KGN cells or GCs.

Objectives

Interestingly, using online bioinformatic tools, we identified that *PAK2* may be regulated by MALAT1 through competitive binding to miR-155-5p. Downregulation of *PAK2* in PCOS ovarian tissues has been shown to trigger oxidative stress via the Nrf2/HO-1 pathway and mediate apoptosis in KGN cells through the β-catenin/c-Myc/PKM2 signaling axis.[19] Additionally, miR-155-5p has been reported to enhance glycolysis in KGN cells, which may be linked to increased cell proliferation.[20] Based on these findings, we hypothesized that MALAT1 may play a regulatory role in the proliferation, apoptosis and ferroptosis of KGN cells through the miR-155-5p/PAK2 axis. This study primarily employed in vitro experiments to validate this hypothesis.

Materials and methods

Bioinformatic analysis

The StarBase online database (https://rnasysu.com/en-cori/agoClipRNA.php?source=lncRNA) was used to predict the binding sites between MALAT1, PAK2 and miR-155-5p. First, the potential binding sites between MALAT1 and miR-155-5p were predicted using the miRNA-Target (lncRNAs) option. Next, the binding sites between miR-155-5p and PAK2 were predicted using the miRNA-Target (mRNA) option.

Cell culture and transfection

The KGN cells (cat. No. CL-0603; Procell, Wuhan, China) were cultured in DMEM/F12 medium supplemented with 10% fetal bovine serum (FBS) in a cell incubator (Thermo Fisher Scientific, Waltham, USA) at 37°C with 5% CO_2. The siRNA targeting MALAT1 (si-MALAT1) and its negative control (si-NC), as well as the miR-155-5p inhibitor and its corresponding control (Ctrl inhibitor), were designed and synthesized by GenePharma (Suzhou, China). Cells

were seeded in 24-well plates, and si-MALAT1, miR-155-5p inhibitor or their respective controls were transfected into KGN cells using Lipofectamine 2000 (cat No. 11668030; Thermo Fisher Scientific). After 48 h, the transfected cells were collected for subsequent experiments.

CCK-8 method

Cells were seeded into 96-well plates at a density of 2,500 cells per well. Each experimental group included at least 3 replicates, along with control wells and blank wells containing culture medium only. On the 2nd day, 10 μL of Cell Counting Kit-8 (CCL-8) working solution (cat. No. G1613; Sevicebio, Wuhan, China) was added to each well containing 90 μL of culture medium. The plates were then incubated for an additional 1.5 h in a cell incubator, after which the optical density (OD) values were measured at a wavelength of 450 nm using a microplate reader (MK; Thermo Fisher Scientific).

Apoptosis analysis

After transfection, cells were collected and centrifuged at 500 g for 5 min at 4°C. Apoptosis was assessed using the Annexin V-FITC/PI Apoptosis Kit (cat No. G1511; Servicebio). The binding buffer was precooled to 4°C and used to resuspend the cells at a density of 3×10^6 cells/mL. To each 100 μL of cell suspension, 5 μL of Annexin V-FITC and 5 μL of propidium iodide (PI) were added. After incubating in the dark at room temperature for 10 min, 400 μL of binding buffer was added. Cell apoptosis was then evaluated using a flow cytometer (CytoFlex; Beckman Coulter, Brea, USA).

RNA extraction

Total RNA was extracted from the cell samples in each group using the TRIzol Kit (cat. No. R0016; Beyotime, Shanghai, China). Briefly, cells were lysed in TRIzol, followed by the addition of 100 μL of chloroform replacement (cat. No. G3014-01; Servicebio) to every 1 mL of RNA extraction mixture. After vortexing for 15 s, the mixture was left at room temperature for 5 min and then centrifuged at 12,000 g for 15 min at 4°C. The upper colorless aqueous phase was carefully transferred to new centrifuge tubes, and total RNA was precipitated using isopropanol. Subsequently, 75% ethanol was added to remove residual salts and isopropanol. The RNA pellet was dissolved in diethylpyrocarbonate (DEPC)-treated water. The concentration and purity of total RNA were measured with ultraviolet spectrophotometry at A260.

Reverse transcription quantitative polymerase chain reaction

The BeyoFast™ SYBR Green One-Step RT-qPCR Kit (cat. No. D7268S; Beyotime) was used to measure the relative

expression of MALAT1, with GAPDH as the internal reference, using total RNA as the template. According to the manufacturer's protocol, a 20 μL reaction system was prepared for each well in a 96-well plate, consisting of 10 μL SYBR Green One-Step Reaction Buffer (×2), 2 μL Enzyme Mix (×10), 2 μL Primer Mix (3 μM each), 2 μL RNA template, and RNase-free water to a final volume of 20 μL. The reverse transcription quantitative polymerase chain reaction (RT-qPCR) cycling conditions were set as follows: reverse transcription at 50°C for 30 min, pre-denaturation at 95°C for 2 min, followed by 40 cycles of denaturation at 95°C for 15 s and annealing/extension at 60°C for 15–30 s. Primers used in this study were synthesized by Sangon Biotech (Shanghai, China) and included the following sequences:

MALAT1 Forward (F):
5'-GCTCTGTGGTGTGGGATTGA-3';
MALAT1 Reverse (R):
5'-GTGGCAAAATGGCGGACTTT-3';
GAPDH Forward (F):
5'-GGTGGTCTCCTCTGACTTCAACA-3';
GAPDH Reverse (R):
5'-CCAAATTCGTTGTCATACCAGGAAATG-3'.

For miR-155-5p, the RT-qPCR analysis was performed using the miRNA 1st Strand cDNA Synthesis Kit (by stem-loop) (cat. No. MR101-01; Vazyme, Beijing, China) and the miRNA Unimodal SYBR qPCR Master Mix Kit (cat. No. MQ102-C1; Vazyme), with U6 as the internal reference. The cDNA synthesis reaction system included 10 μL RNA template, 1 μL RT primer (2 μM), 2 μL RT Mix, 2 μL HiScript II Enzyme Mix, and RNase-free ddH$_2$O to the final volume. The reaction was carried out under the following conditions: 25°C for 5 min, 50°C for 15 min and 85°C for 5 min. The RT primer used for miR-155-5p was 5'-GTCGTATCCAGTGCAGGGTCCGAGGTATTCG-CACTGGATACGACAACCCC-3'. The qPCR primers for miR-155-5p were:

Forward (F): 5'-CGCGTTAATGCTAATCGTGATA-3';
Reverse (R): 5'-AGTGCAGGGTCCGAGGTATT-3'.

The qPCR reaction system consisted of 10 μL 2× miRNA Unimodal SYBR qPCR Master Mix, 0.4 μL forward primer, 0.4 μL reverse primer, 2 μL cDNA template, and RNase-free ddH$_2$O to the final volume. The qPCR cycling conditions were as follows: 95°C for 10 s, followed by 40 cycles of 95°C for 10 s and 60°C for 30 s. Relative expression levels were analyzed using the $2^{-\Delta\Delta CT}$ method in Microsoft Excel 2013 (Microsoft Corp., Redmond, USA).

Western blot

Total proteins were extracted using RIPA with supplementation of phenylmethylsulfonyl fluoride (PMSF) on ice (cat. No. P0013B; Beyotime). The protein concentration was determined using bicinchoninic acid (BCA) kit (Bioss, Beijing, China). Then 5 × loading buffer was added and the protein samples were boiled for 20 min. Sodium dodecyl

sulfate–polyacrylamide gel electrophoresis (SDS-PAGE) method was used to separate the proteins. The proteins on the gel were then transferred onto polyvinylidene difluoride (PVDF) membranes. Tris-buffered saline with Tween (TBST) was used to dilute the skim milk to 5%, which was then used to block the membranes for 1 h at 37°C. The primary antibodies were diluted using TBST at 1:1,000, which included the anti-GPX4 (cat. No. bs-3884R; Bioss), anti-SLC7A11(cat. No. bs-6883R; Bioss) and anti-PAK2 (cat. No. 19979-1-AP; Proteintech, Wuhan, China). The anti-GAPDH was diluted at 1:10,000 (cat. No. bs-10900R; Bioss). The primary antibodies were used to incubate the membranes for 1 h at 37°C. TBST was used to wash the membranes for 3 times, 5 min each time. The secondary antibody (cat. No. AB0101; Abways, Shanghai, China) was diluted at 1 : 20,000 using TBST and was used to incubate the membranes for 1 h at room temperature. The membranes were washed using TBST 3 times, 8 min each time. The eclectrochemiluminescence (ECL) kit was applied onto the membranes, and the immunoblotting image was taken on an ECL imaging machine (Servicebio). ImageJ (National Institutes of Health (NIH), Bethesda, USA) was used to analyze the grey values.

Dual-luciferase reporter gene assays

Plasmids containing the wild-type and mutant sequences of MALAT1 (MALAT1-wt, MALAT1-mt) and *PAK2* (*PAK2*-wt, *PAK2*-mt) were constructed using the pmiR-GLO vector (Promega, Madison, USA). The KGN cells were transfected with MALAT1-wt/mt or PAK2-wt/mt along with either the miR-155-5p inhibitor or control inhibitor using Lipofectamine 2000. The Dual Luciferase Reporter Assay Kit (cat. No. RG028; Beyotime) was used following the manufacturer's instructions, and dual luciferase activity was measured using a laboratory luminometer.

Analysis of MDA and GSH/GSSG ratios

The MDA Kit (cat. No. S0131S; Beyotime) and the GSH/GSSG Ratio Detection Kit (cat. No. S0053; Beyotime) were used following the standard procedures provided by the manufacturer. Briefly, malondialdehyde (MDA) levels were measured colorimetrically at 532 nm using a laboratory spectrophotometer, according to the product instructions. Total glutathione levels and reduced glutathione (GSH) levels were measured on a microplate reader at 405 nm. Oxidized GSH levels were calculated by subtracting the measured GSH levels from the total glutathione levels.

Statistical analyses

A non-normal distribution was assumed due to the small sample size. Briefly, the statistical significance of differences was assessed using the Kruskal–Wallis test with Dunn's post hoc analysis for multiple group comparisons and the Mann–Whitney U test for two-group comparisons, performed using GraphPad Prism 8 (GraphPad Software, San Diego, USA). Statistical analysis results were presented in the supplementary tables. All experiments were performed in triplicate. Basic calculations, including relative expression levels, protein expression, and luciferase activity, were conducted using Microsoft Excel 2013 (Microsoft Corp.). Figures were generated using Graph-Pad, with triplicate data displayed as scatter plots showing the median and range. A $p < 0.05$ was considered statistically significant.

Results

Downregulation of MALAT1 is associated with increased apoptosis and ferroptosis in KGN cells

We confirmed using RT-qPCR that MALAT1 expression was significantly reduced in KGN cells transfected with siRNA targeting MALAT1, showing a fold change (Fc) of 0.320 ±0.040 (Fig. 1A). Downregulation of MALAT1 reduced cell viability and induced apoptosis in KGN cells (Fig. 1B–E). Additionally, MALAT1 knockdown increased MDA content and decreased the GSH/GSSG ratio in KGN cells (Fig. 2A,B).

Western blot analysis was performed to assess changes in the relative protein expression levels of the anti-ferroptosis markers SLC7A11 and GPX4. The results showed that knockdown of MALAT1 significantly inhibited the expression of both SLC7A11 and GPX4 in KGN cells (Fig. 2C–E). Taken together, these findings indicate that MALAT1 knockdown induces both apoptosis and ferroptosis while reducing cell viability in KGN cells. Furthermore, MALAT1 was found to modulate PAK2 expression in KGN cells by competitively acting as a molecular sponge for miR-155-5p. Bioinformatic analysis using the StarBase online database predicted the binding sites between MALAT1/PAK2 and miR-155-5p (Fig. 3A,B). Based on the predicted binding sites, pmiRGLO plasmids containing MALAT1-wt/mt and PAK2-wt/mt were constructed. Dual-luciferase activity assays were performed after KGN cells were transfected with MALAT1-wt/mt or PAK2-wt/mt along with either the miR-155-5p inhibitor or control inhibitor. The results revealed that relative luciferase activity was significantly enhanced in cells transfected with MALAT1-wt and miR-155-5p inhibitor (Fig. 3C) and was similarly increased in cells transfected with PAK2-wt and miR-155-5p inhibitor (Fig. 3D). These findings verified the direct binding interactions between MALAT1/PAK2 and miR-155-5p in KGN cells. Furthermore, downregulation of MALAT1 in KGN cells led to a significant increase in miR-155-5p expression (fold change, 2.39 ±0.22; Fig. 3E). Inhibition of miR-155-5p increased PAK2 mRNA expression (fold change, 1.94 ±0.15; Fig. 3F) as well as PAK2 protein levels
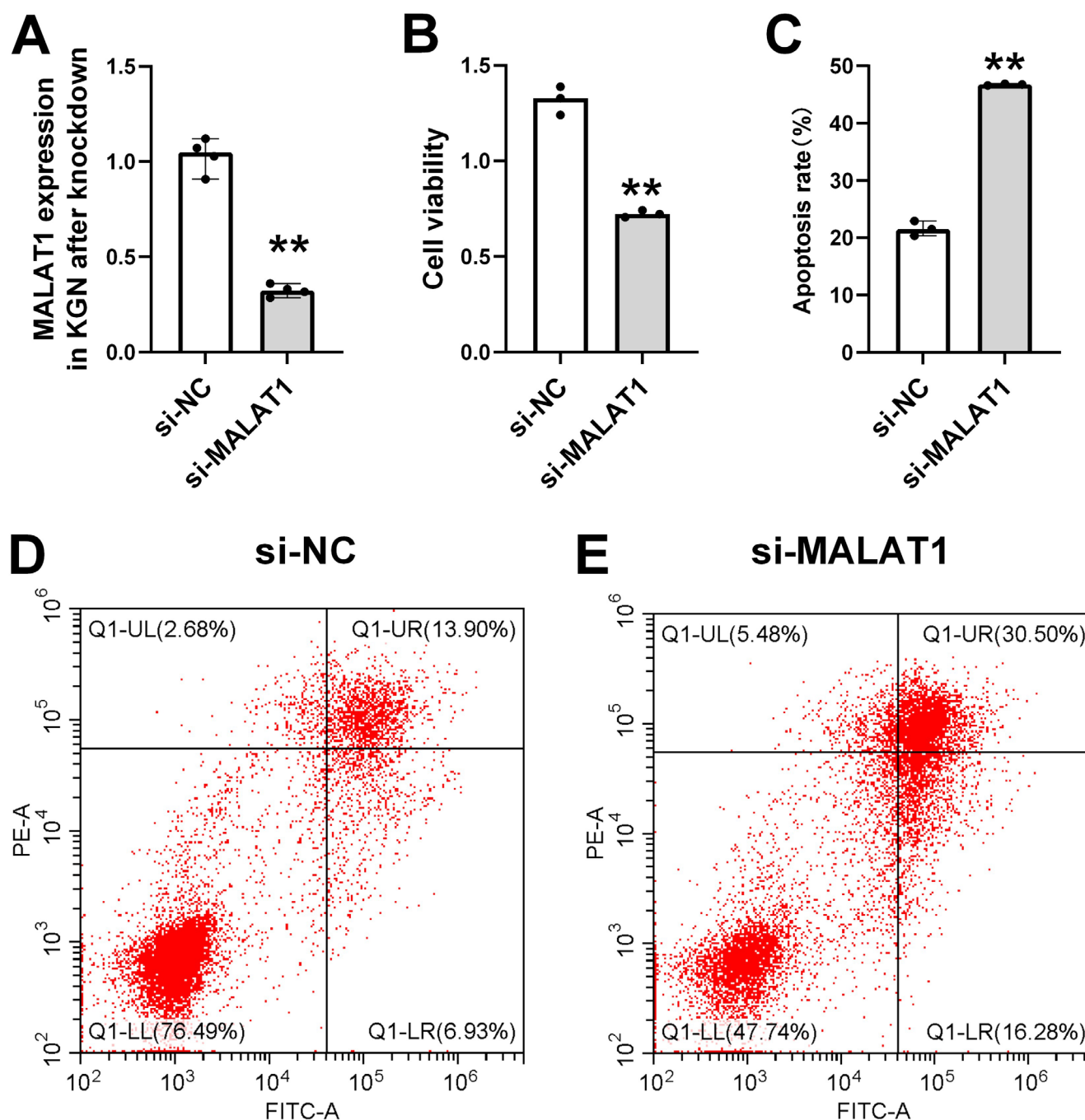
Fig. 1. Downregulation of MALAT1 is associated with apoptosis and ferroptosis in human granulosa cell line (KGN cells). KGN cells were transfected with siRNA targeting MALAT1 (si-MALAT1) and its control (si-NC). A. Cells were collected for reverse transcription quantitative polymerase chain reaction (RT-qPCR) analysis; B. Cell viability assessment; C–E. Apoptosis analysis. The statistical significance of differences was analyzed using the Kruskal–Wallis test with Dunn's post hoc for multiple group comparisons, and the Mann–Whitney U test for comparisons between 2 groups. Data are presented as scatter plots with median and range lines; $p < 0.05$ was considered statistically significant

(Fig. 4B). The mRNA expression level of PAK2 was suppressed by MALAT1 knockdown (fold change, 0.49 ±0.05) but was restored by co-treatment with the miR-155-5p inhibitor (fold change, 0.92 ±0.07) in KGN cells (Fig. 4A. Similarly, MALAT1 knockdown reduced PAK2 protein levels, which were reversed upon miR-155-5p inhibition (Fig. 4A,C). Taken together, these results demonstrate that MALAT1 regulates PAK2 expression by competitively binding to miR-155-5p.

miR-155-5p downregulation enhances cell viability and inhibits apoptosis and ferroptosis

Inhibition of miR-155-5p significantly increased cell viability and reduced apoptosis in KGN cells (Fig. 5). Additionally, downregulation of miR-155-5p decreased MDA content, increased the GSH/GSSG ratio, and elevated the protein expression levels of GPX4 and SLC7A11
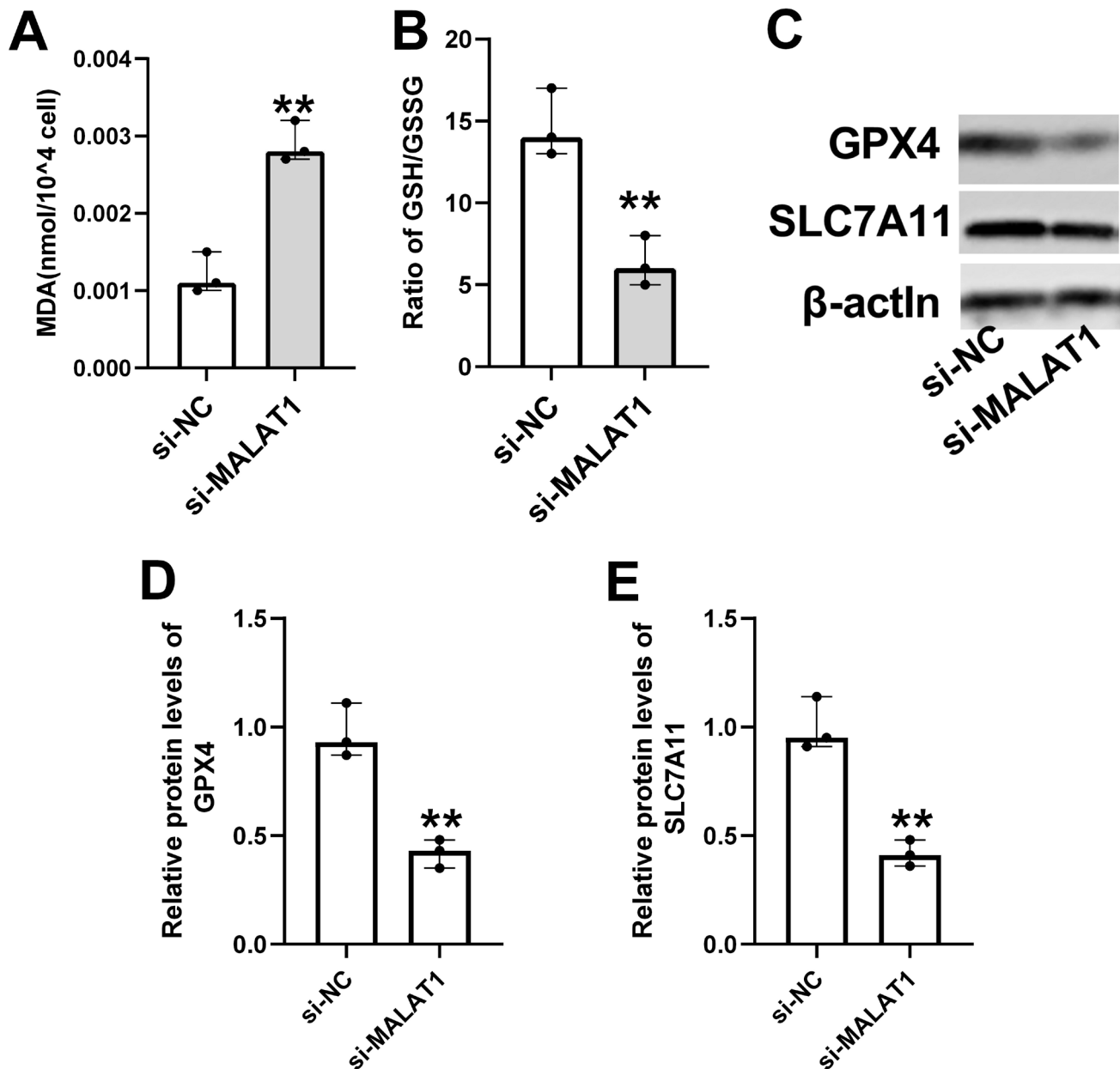
Fig. 2. Downregulation of MALAT1 is associated with ferroptosis in human granulosa cell line (KGN cells). A,B. MDA content and GSH/GSSG ratio; C–E. Western blot experiments and ImageJ analysis were used to assess the protein expression levels of SLC7A11 and GPX4. The statistical significance of differences was analyzed using the Kruskal–Wallis test with Dunn's post hoc for multiple group comparisons and the Mann–Whitney U test for comparisons between 2 groups. Data are presented as scatter plots with median and range lines; $p < 0.05$ was considered statistically significant

MDA – malondialdehyde; GSH – reduced glutathione; GSSG – oxidized glutathione disulfide.

in KGN cells (Fig. 6), suggesting that miR-155-5p downregulation also reduces ferroptosis in KGN cells.

Downregulation of miR-155-5p reverses the impacts of MALAT1 knockdown in KGN cells

As described above, knockdown of MALAT1 reduced cell viability and induced apoptosis and ferroptosis in KGN cells. We further validated that inhibition of miR-155-5p could reverse the effects of MALAT1 knockdown in these cells (Fig. 7). Specifically, the reduction in cell viability

caused by MALAT1 knockdown was restored by miR-155-5p downregulation (Fig. 7A), and the increase in apoptosis induced by MALAT1 knockdown was reversed by miR-155-5p inhibition (Fig. 7B–E). The increase in MDA content induced by MALAT1 knockdown was reversed by miR-155-5p inhibition (Fig. 8A). Similarly, the reductions in the GSH/GSSG ratio and the relative protein expression levels of GPX4 and SLC7A11 caused by MALAT1 knockdown in KGN cells were restored by downregulation of miR-155-5p (Fig. 8B–E). These findings demonstrate that miR-155-5p inhibition can effectively reverse the impacts of MALAT1 knockdown in KGN cells.
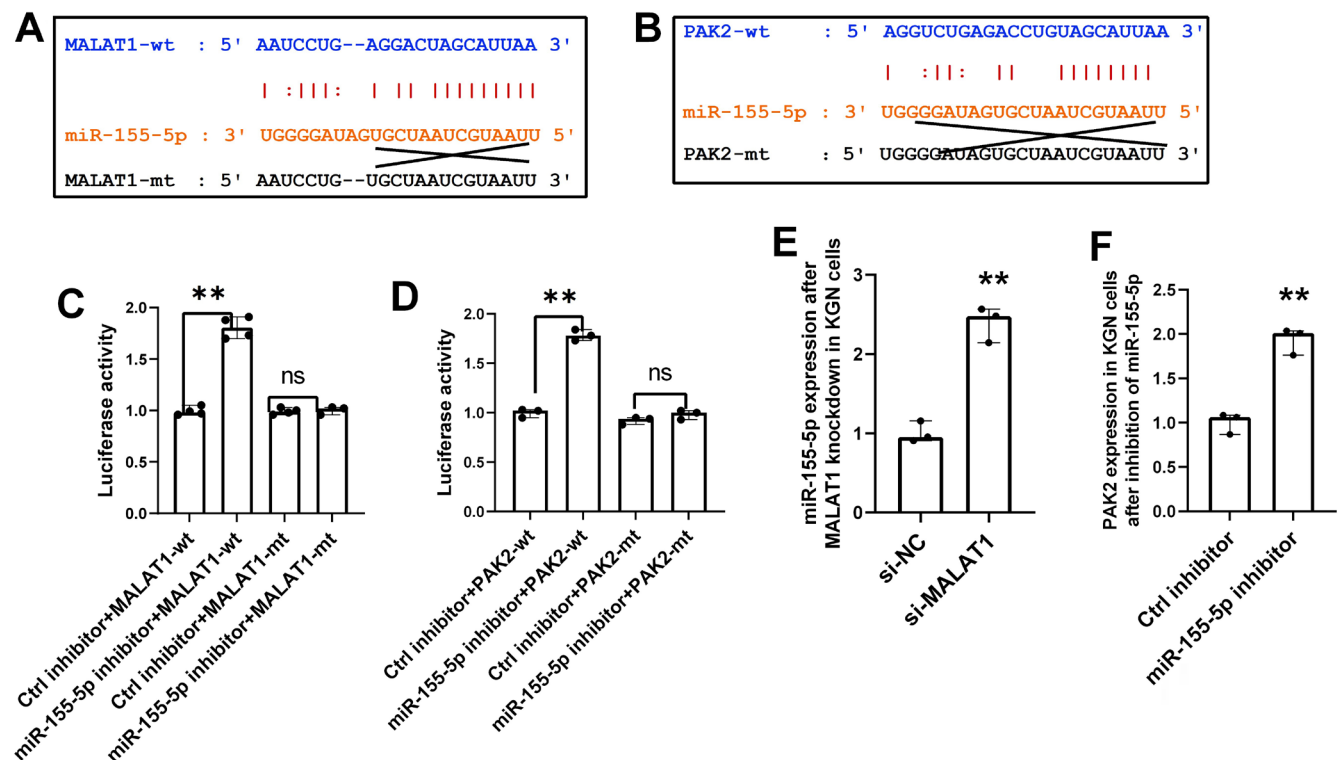
Fig. 3. MALAT1 sponges miR-155-5p and targets PAK2 in human granulosa cell line (KGN cells). A,B. Bioinformatic analysis was conducted using the StarBase online database (https://rnasysu.com/encori/agoClipRNA.php?source=lncRNA) to predict the targeting sites between miR-155-5p and MALAT1/PAK2; C,D. Dual-luciferase reporter assays were performed to examine the relative luciferase activity; E. Relative expression of miR-155-5p in KGN cells following MALAT1 knockdown; F. PAK2 expression in KGN cells after inhibition of miR-155-5p
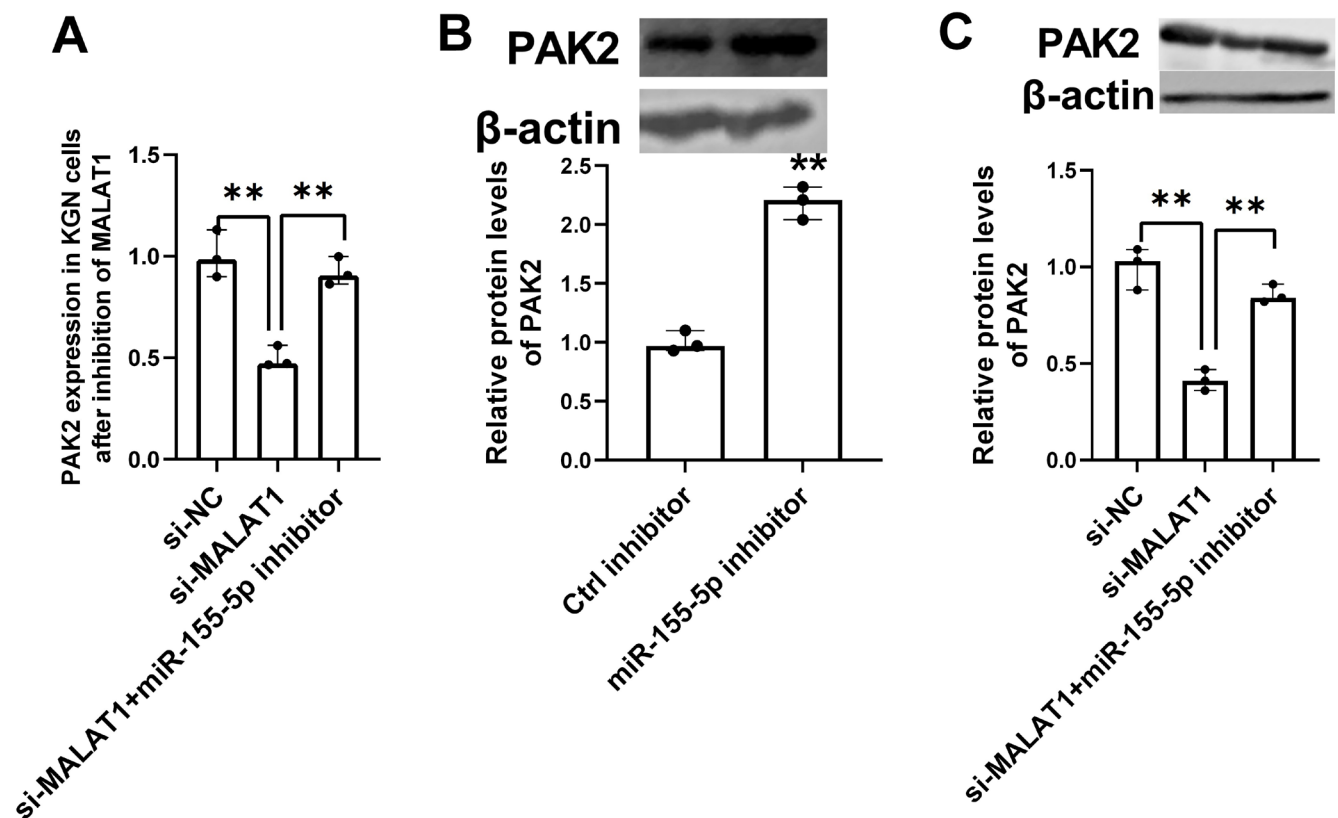

Fig. 4. *PAK1* is inhibited by knockdown of MALAT1 and restored by miR-155-5p inhibitor in human granulosa cell line (KGN cells). A. PAK2 expression in KGN cells after MALAT1 knockdown or MALAT1 knockdown combined with miR-155-5p inhibition; B,C. Relative protein expression levels of PAK2; $p < 0.05$ was considered statistically significant
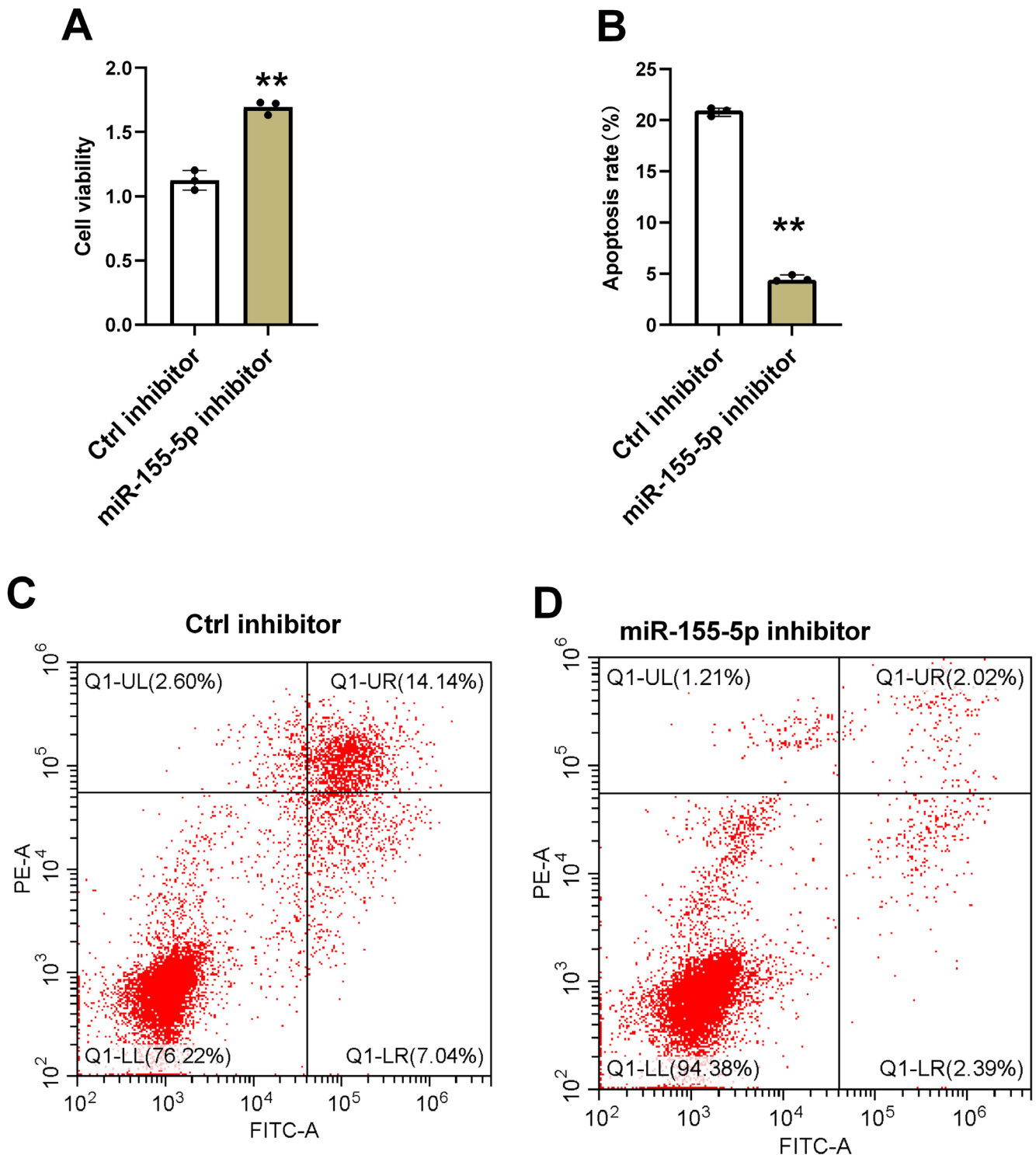
Fig. 5. miR-155-5p downregulation enhances cell viability and inhibits apoptosis and ferroptosis. Human granulosa cell line (KGN cells) were transfected with the miR-155-5p inhibitor or its control (Ctrl inhibitor). A. Cell viability; B–D. Cell apoptosis analysis; p < 0.05 was considered statistically significant

Discussion

The significance of this study lies in its investigation of MALAT1's role in regulating apoptosis and ferroptosis in KGN cells, providing new insights into the pathophysiology of PCOS. Prior research has shown that MALAT1 downregulation is associated with increased apoptosis and decreased proliferation in GCs, contributing to ovary dysfunction in PCOS.[15,21] Abnormal GC death, particularly through apoptosis, has been identified as a key factor driving disrupted folliculogenesis in PCOS, ultimately leading to anovulation and infertility.[22] Ferroptosis, a relatively
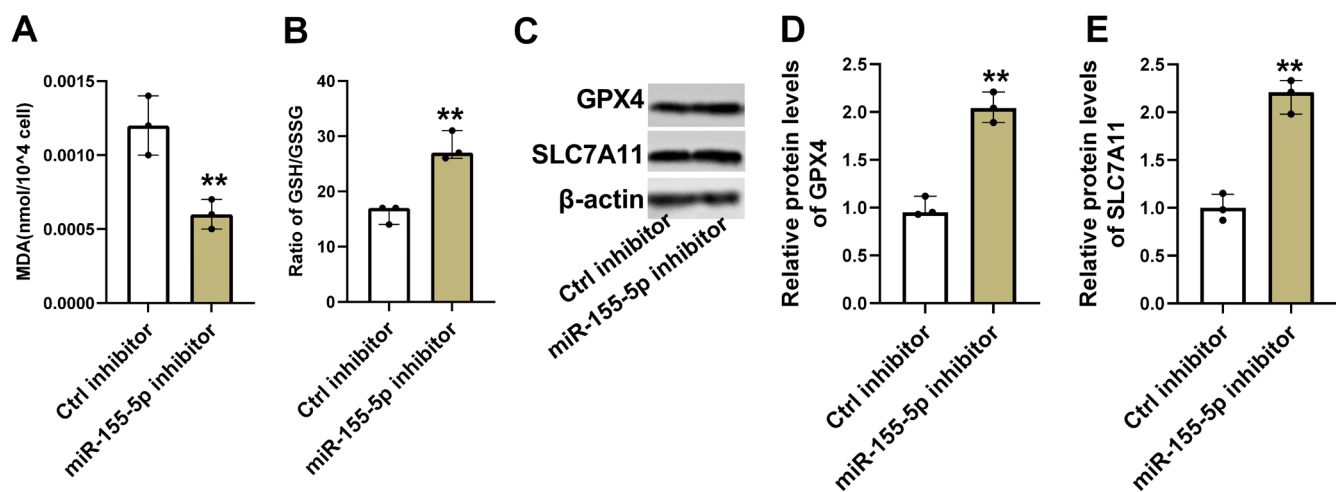
Fig. 6. miR-155-5p downregulation inhibits ferroptosis. A,B. MDA levels and GSH/GSSG ratios; C–E. Relative protein expression of the anti-ferroptosis markers SLC7A11 and GPX4; p < 0.05 was considered statistically significant

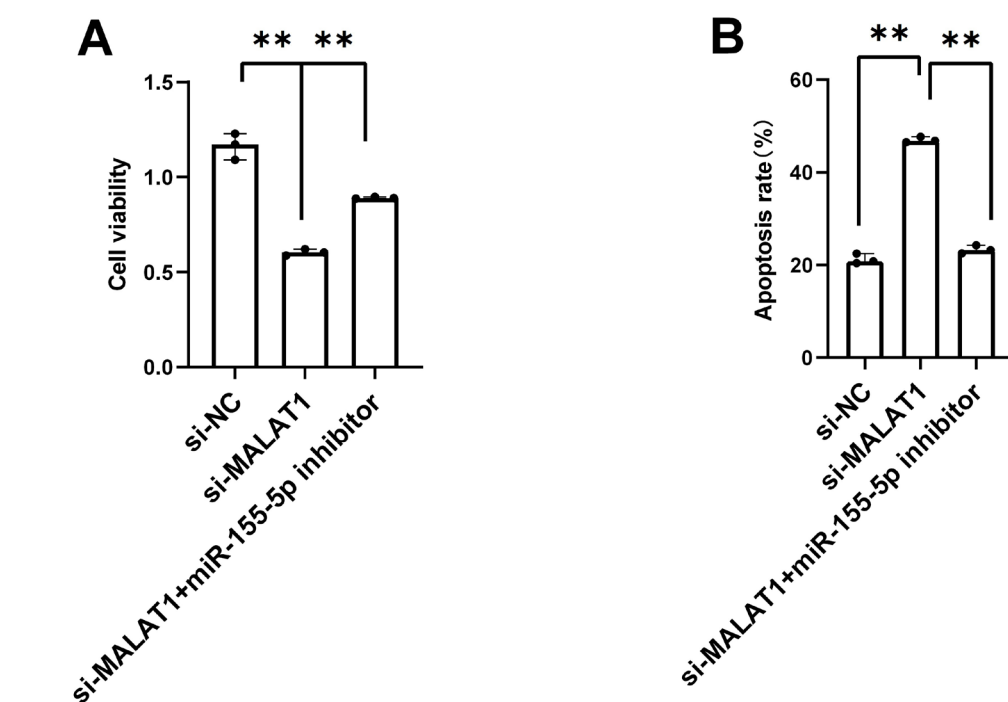MDA – malondialdehyde; GSH – reduced glutathione; GSSG – oxidized glutathione disulfide.

Fig. 7. Downregulation of miR-155-5p reverses the impact of MALAT1 knockdown on cell apoptosis. Human granulosa cell line (KGN cells) cells were transfected with si-NC, si-MALAT1 or si-MALAT1 combined with miR-155-5p inhibitor.
A–C. Cell viability and apoptosis measurements; p < 0.05 was considered statistically significant

A

B

C

D

E

Fig. 8. Downregulation of miR-155-5p reverses the impact of MALAT1 knockdown on cell ferroptosis. A,B. MDA levels and GSH/GSSG ratios; C–E. Relative protein expression of the anti-ferroptosis markers SLC7A11 and GPX4; $p < 0.05$ was considered statistically significant

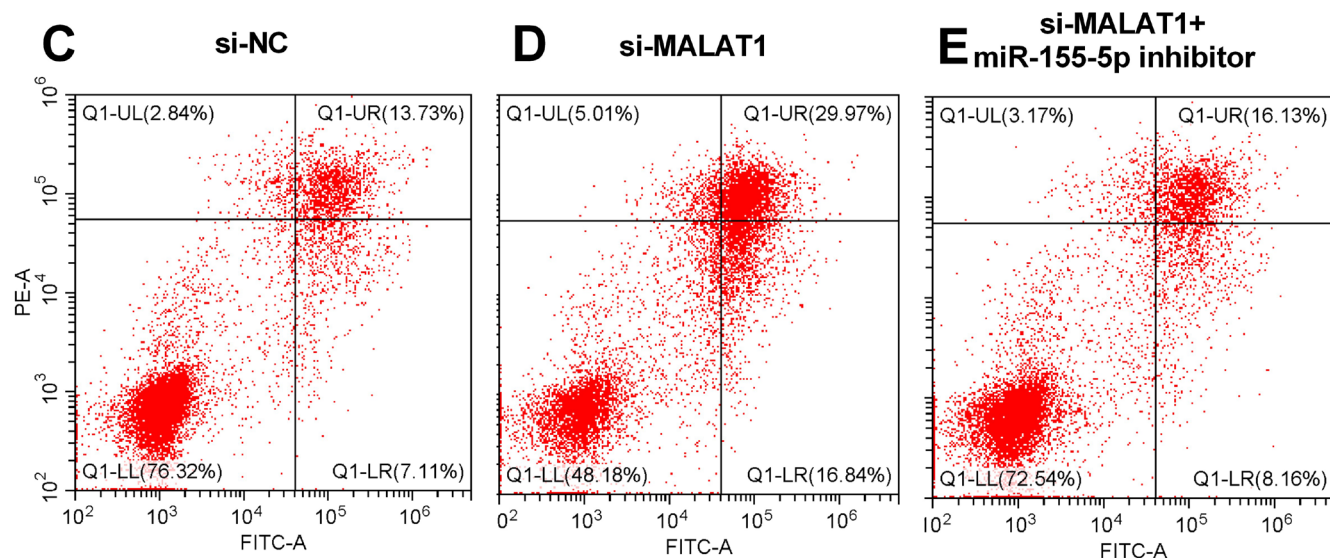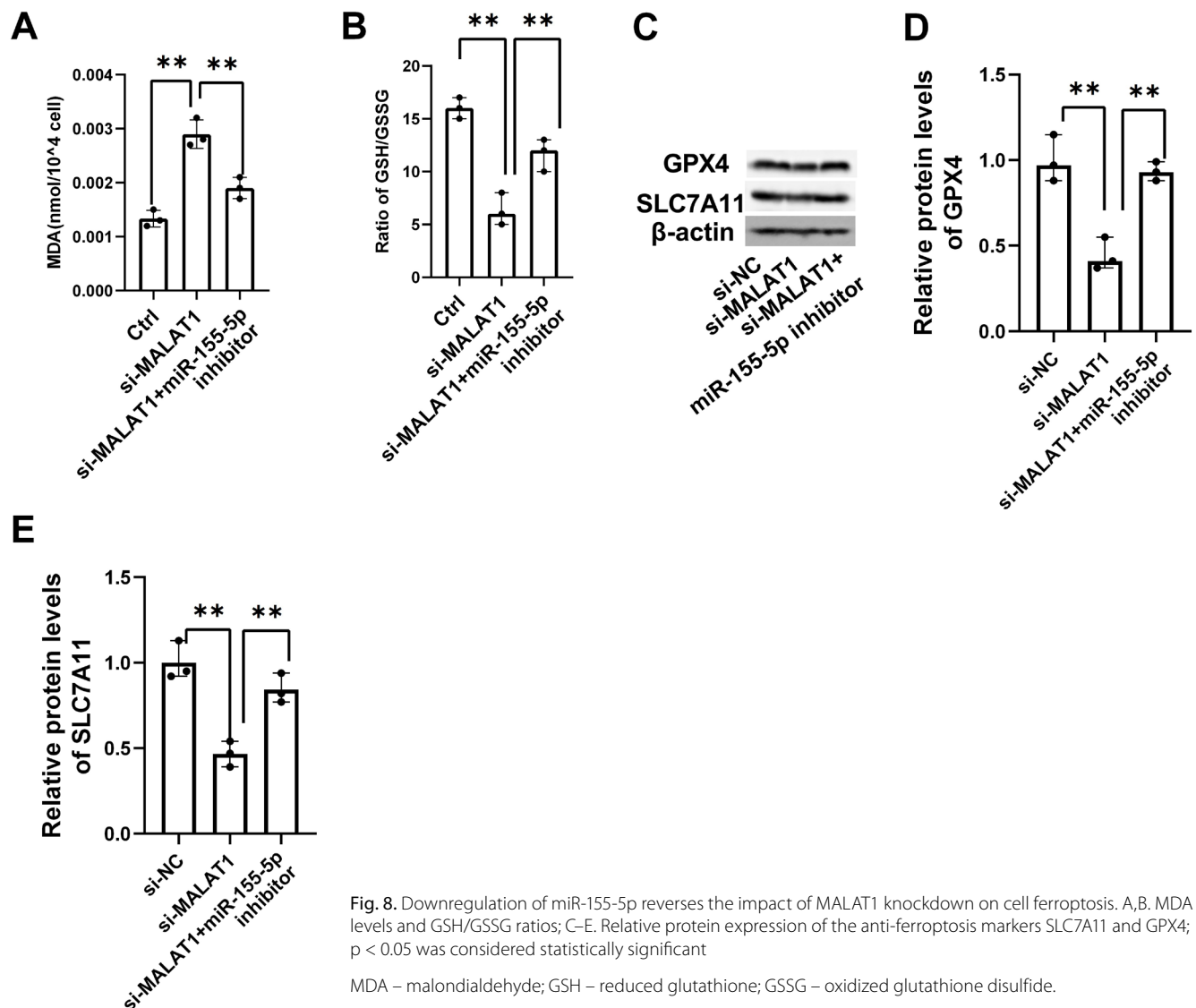MDA – malondialdehyde; GSH – reduced glutathione; GSSG – oxidized glutathione disulfide.

newly characterized form of programmed cell death distinct from apoptosis, is marked by iron-dependent lipid peroxidation.[21,23] In recent years, studies have found that ferroptosis-related genes are dysregulated in GCs from PCOS patients and that inhibition of ferroptosis can alleviate PCOS symptoms in animal models.[7,21] Interestingly, another study reported that MALAT1 knockdown promotes ferroptosis in ectopic endometrial stromal cells in endometriosis, suggesting a potential connection between MALAT1 and ferroptosis regulation.[24]

In PCOS, ferroptosis-related genes have been linked to impaired oocyte quality.[25] Enhanced ferroptosis in ovarian GCs from PCOS patients is associated with oocyte dysmaturity, increasing the risk of infertility.[26] GPX4 acts as a key antioxidant regulator of ferroptosis by reducing reactive oxygen species (ROS) accumulation and enhancing cellular resistance to ferroptosis.[27] Additionally, GSH is synthesized from cysteine via the System Xc⁻ (comprising SLC7A11 and SLC3A2) and the transsulfuration pathway, with GSH consumption leading to GPX4 inactivation.[28] SLC7A11, an upstream modulator of ferroptosis,

inhibits lipid peroxidation accumulation and protects cells from ferroptosis by increasing cysteine availability and facilitating GSH synthesis.[29]

Recent studies have begun exploring ferroptosis-related regulatory mechanisms in PCOS using both cell and animal models. For example, PPAR-α has been shown to inhibit ferroptosis in GCs by interacting with FADS2, reducing MDA levels, and increasing GSH and GPX4 expression.[23] miR-93-5p has been identified as a potential target in PCOS, as it can promote apoptosis and ferroptosis in GCs.[30,31] However, to date, no studies have specifically examined the role of MALAT1 in ferroptosis regulation within the context of PCOS. In this study, we demonstrated that downregulation of MALAT1 in KGN cells reduces GSH, GPX4 and SLC7A11 levels, thereby promoting ferroptosis. This reveals a previously uncharacterized ferroptosis-related function of MALAT1 in the pathophysiology of PCOS in vitro. Furthermore, our research builds on previous findings by elucidating a novel MALAT1/miR-155-5p/PAK2 regulatory axis in KGN cells, expanding the understanding of MALAT1's role as a competing

endogenous RNA (ceRNA). While the ceRNA function of MALAT1 has been established in various biological contexts, e.g., sponging miR-211-5p to regulate FOXO3 in H_2O_2-induced GCs,[32] regulating the MALAT1/miR-212-5p/MyD88 axis in osteoarthritis,[33] and controlling the MALAT1/miR-216a-5p/FOXA1 pathway in prostate cancer,[34] our study is the first to report MALAT1's modulation of miR-155-5p and its downstream effects on PAK2 in KGN cells.

Previous studies have shown that miR-155-5p is differentially expressed in follicular fluid exosomes from PCOS patients and is involved in glycolysis-related pathways in KGN cells, potentially influencing cell proliferation and apoptosis.[20] Additionally, *PAK2* has been shown to upregulate PKM2, a key glycolysis indicator, thereby mediating cell proliferation.[30] In the context of PCOS, PAK2 has been implicated in regulating KGN cell apoptosis and proliferation via the β-catenin/c-Myc/PKM2 signaling pathway.[19,35] *PAK2* regulates glycolytic processes and cell proliferation through the β-catenin/c-Myc/PKM2 signaling pathway in PCOS, underscoring the importance of altered glucose metabolism in the pathological mechanisms driving PCOS development.

Limitations

This study has several limitations. Obtained in vitro, our findings may not fully capture the complex conditions within the ovary environment in vivo, limiting their direct applicability to PCOS. Additionally, while we examined apoptosis and ferroptosis, other cell death pathways, such as autophagy, might also play roles in GC dysfunction. Lastly, the absence of clinical validation means the relevance of MALAT1 as a therapeutic target remains uncertain. Future studies should use in vivo models and patient samples to confirm these results.

Conclusions

This study reveals that MALAT1 regulates apoptosis and ferroptosis in KGN cells through the miR-155-5p/*PAK2* pathway, providing new insights into GC dysfunction in PCOS. Our findings highlight MALAT1 as a potential therapeutic target, suggesting that targeting the MALAT1/miR-155-5p/*PAK2* axis could mitigate cellular damage in PCOS. Further research in animal models and clinical settings is needed to validate these findings and explore MALAT1's potential as a treatment target.

Supplementary data

The supplementary materials are available at https://doi.org/10.5281/zenodo.14872220. The package includes the following files:

Supplementary Table 1. Mann–Whitney U test results.

Supplementary Table 2. Results of Kruskal–Wallis test with Dunn's post hoc test.

Data availability

The datasets generated and/or analyzed during the current study are available from the corresponding author on reasonable request.
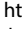
Consent for publication

Not applicable.

Use of AI and AI-assisted technologies

Not applicable.

ORCID iDs

Yun Yang ⓘ https://orcid.org/0009-0002-6763-0958
Dan Li ⓘ https://orcid.org/0009-0008-2403-4746
Lu Sun ⓘ https://orcid.org/0009-0008-5956-2063
Shasha Liu ⓘ https://orcid.org/0000-0001-6516-7168

References

1. Wang Z, Jukic AMZ, Baird DD, et al. Irregular cycles, ovulatory disorders, and cardiometabolic conditions in a US-based digital cohort. *JAMA Netw Open*. 2024;7(5):e249657. doi:10.1001/jamanetworkopen.2024.9657
2. Teede HJ, Tay CT, Laven JJE, et al. Recommendations from the 2023 International Evidence-based Guideline for the Assessment and Management of Polycystic Ovary Syndrome. *J Clin Endocrinol Metab*. 2023;108(10):2447–2469. doi:10.1210/clinem/dgad463
3. Yang J, Chen C. Hormonal changes in PCOS. *J Endocrinol*. 2024;261(1):e230342. doi:10.1530/JOE-23-0342
4. Joshi A. PCOS stratification for precision diagnostics and treatment. *Front Cell Dev Biol*. 2024;12:1358755. doi:10.3389/fcell.2024.1358755
5. Hesampour A, Jafarabadi M, Rajabi S, Rezayof E, Nezamabadi AG. Dual oxidase 1, 2 gene expression in women with polycystic ovary syndrome (PCOS). *J Fam Reprod Health*. 2023;17(4):205–215. doi:10.18502/jfrh.v17i4.14592
6. Zhou J, Liu F, Tian L, et al. Mutational analysis of minichromosome maintenance complex component (*MCM*) family genes in Chinese Han women with polycystic ovarian syndrome. *Gynecol Endocrinol*. 2023;39(1):2206912. doi:10.1080/09513590.2023.2206912
7. Li X, Lin Y, Cheng X, et al. Ovarian ferroptosis induced by androgen is involved in pathogenesis of PCOS. *Hum Reprod Open*. 2024;2024(2):hoae013. doi:10.1093/hropen/hoae013
8. Zhou Z, Zhang Y, Tan C, et al. The long non-coding RNA BBOX1 antisense RNA 1 is upregulated in polycystic ovary syndrome (PCOS) and suppresses the role of microRNA-19b in the proliferation of ovarian granulose cells. *BMC Womens Health*. 2023;23(1):508. doi:10.1186/s12905-023-02632-5
9. Li X, Zhu L, Luo Y. Long non-coding RNA HLA-F antisense RNA 1 inhibits the maturation of microRNA-613 in polycystic ovary syndrome to promote ovarian granulosa cell proliferation and inhibit cell apoptosis. *Bioengineered*. 2022;13(5):12289–12297. doi:10.1080/21655979.2022.2070965
10. ElMonier AA, El-Boghdady NA, Fahim SA, Sabry D, Elsetohy KA, Shaheen AA. LncRNA NEAT1 and MALAT1 are involved in polycystic ovary syndrome pathogenesis by functioning as competing endogenous RNAs to control the expression of PCOS-related target genes. *Noncoding RNA Res*. 2023;8(2):263–271. doi:10.1016/j.ncrna.2023.02.008
11. Li S, Li Y, Yan X, et al. MALAT1 expression in granulosa cells in PCOS patients with different phenotypes. *Sci Rep*. 2024;14(1):5019. doi:10.1038/s41598-024-55760-9

12. Zhang D, Tang HY, Tan L, Zhao DM. MALAT1 is involved in the patho-physiological process of PCOS by modulating TGFβ signaling in granulosa cells. *Mol Cell Endocrinol*. 2020;499:110589. doi:10.1016/j.mce.2019.110589

13. Tu M, Wu Y, Wang F, et al. Effect of lncRNA MALAT1 on the granulosa cell proliferation and pregnancy outcome in patients with PCOS. *Front Endocrinol (Lausanne)*. 2022;13:825431. doi:10.3389/fendo.2022.825431

14. Chen Y, Chen Y, Cui X, He Q, Li H. Down-regulation of MALAT1 aggravates polycystic ovary syndrome by regulating MiR-302d-3p-mediated leukemia inhibitory factor activity. *Life Sci*. 2021;277:119076. doi:10.1016/j.lfs.2021.119076

15. Li Y, Xiang Y, Song Y, Zhang D, Tan L. MALAT1 downregulation is associated with polycystic ovary syndrome via binding with MDM2 and repressing P53 degradation. *Mol Cell Endocrinol*. 2022;543:111528. doi:10.1016/j.mce.2021.111528

16. Peiyin F, Yuxian W, Jiali Z, Jian X. Research progress of ferroptosis in female infertility. *J Ovarian Res*. 2024;17(1):183. doi:10.1186/s13048-024-01508-y

17. Wang M, Zhang BQ, Ma S, et al. Broadening horizons: The role of ferroptosis in polycystic ovary syndrome. *Front Endocrinol (Lausanne)*. 2024;15:1390013. doi:10.3389/fendo.2024.1390013

18. Li YY, Peng YQ, Yang YX, et al. Baicalein improves the symptoms of polycystic ovary syndrome by mitigating oxidative stress and ferroptosis in the ovary and gravid placenta. *Phytomedicine*. 2024;128:155423. doi:10.1016/j.phymed.2024.155423

19. Hui M, Hu S, Ye L, Zhang M, Jing X, Hong Y. PAK2/beta-catenin/c-Myc/PKM2 signal transduction suppresses ovarian granulosa cell apoptosis in polycystic ovary syndrome. *Biochem Biophys Res Commun*. 2023;677:54–62. doi:10.1016/j.bbrc.2023.08.004

20. Cao J, Huo P, Cui K, et al. Follicular fluid-derived exosomal miR-143-3p/miR-155-5p regulate follicular dysplasia by modulating glycolysis in granulosa cells in polycystic ovary syndrome. *Cell Commun Signal*. 2022;20(1):61. doi:10.1186/s12964-022-00876-6

21. Yao Y, Wang B, Jiang Y, Guo H, Li Y. The mechanisms crosstalk and therapeutic opportunities between ferroptosis and ovary diseases. *Front Endocrinol (Lausanne)*. 2023;14:1194089. doi:10.3389/fendo.2023.1194089

22. Escobar-Morreale HF. Polycystic ovary syndrome: Definition, aetiology, diagnosis and treatment. *Nat Rev Endocrinol*. 2018;14(5):270–284. doi:10.1038/nrendo.2018.24

23. Liu Y, Ni F, Huang J, et al. PPAR-α inhibits DHEA-induced ferroptosis in granulosa cells through upregulation of FADS2. *Biochem Biophys Res Commun*. 2024;715:150005. doi:10.1016/j.bbrc.2024.150005

24. Liang Z, Wu Q, Wang H, et al. Silencing of lncRNA MALAT1 facilitates erastin-induced ferroptosis in endometriosis through miR-145-5p/MUC1 signaling. *Cell Death Discov*. 2022;8(1):190. doi:10.1038/s41420-022-00975-w

25. Huang J, Fan H, Li C, et al. Dysregulation of ferroptosis-related genes in granulosa cells associates with impaired oocyte quality in polycystic ovary syndrome. *Front Endocrinol (Lausanne)*. 2024;15:1346842. doi:10.3389/fendo.2024.1346842

26. Ni Z, Li Y, Song D, et al. Iron-overloaded follicular fluid increases the risk of endometriosis-related infertility by triggering granulosa cell ferroptosis and oocyte dysmaturity. *Cell Death Dis*. 2022;13(7):579. doi:10.1038/s41419-022-05037-8

27. Forcina GC, Dixon SJ. GPX4 at the crossroads of lipid homeostasis and ferroptosis. *Proteomics*. 2019;19(18):1800311. doi:10.1002/pmic.201800311

28. Sun Y, Chen P, Zhai B, et al. The emerging role of ferroptosis in inflammation. *Biomed Pharmacother*. 2020;127:110108. doi:10.1016/j.biopha.2020.110108

29. Ye Z, Liu W, Zhuo Q, et al. Ferroptosis: Final destination for cancer? *Cell Prolif*. 2020;53(3):e12761. doi:10.1111/cpr.12761

30. Gupta A, Ajith A, Singh S, Panday RK, Samaiya A, Shukla S. PAK2–c-Myc–PKM2 axis plays an essential role in head and neck oncogenesis via regulating Warburg effect. *Cell Death Dis*. 2018;9(8):825. doi:10.1038/s41419-018-0887-0

31. Tan W, Dai F, Yang D, et al. MiR-93-5p promotes granulosa cell apoptosis and ferroptosis by the NF-kB signaling pathway in polycystic ovary syndrome. *Front Immunol*. 2022;13:967151. doi:10.3389/fimmu.2022.967151

32. Zhang M, Xing J, Zhao S, et al. Exosomal YB-1 facilitates ovarian restoration by MALAT1/miR-211-5p/FOXO3 axis. *Cell Biol Toxicol*. 2024;40(1):29. doi:10.1007/s10565-024-09871-8

33. Gao Z, Guo C, Xiang S, Zhang H, Wang Y, Xu H. Suppression of MALAT1 promotes human synovial mesenchymal stem cells enhance chondrogenic differentiation and prevent osteoarthritis of the knee in a rat model via regulating miR-212-5p/MyD88 axis. *Cell Tissue Res*. 2024;395(3):251–260. doi:10.1007/s00441-024-03863-0

34. Zeng F, Li D, Kang X, et al. MALAT1 promotes FOXA1 degradation by competitively binding to miR-216a-5p and enhancing neuroendocrine differentiation in prostate cancer. *Transl Oncol*. 2024;39:101807. doi:10.1016/j.tranon.2023.101807

35. Liang A, Zhang W, Wang Q, et al. Resveratrol regulates insulin resistance to improve the glycolytic pathway by activating SIRT2 in PCOS granulosa cells. *Front Nutr*. 2023;9:1019562. doi:10.3389/fnut.2022.1019562